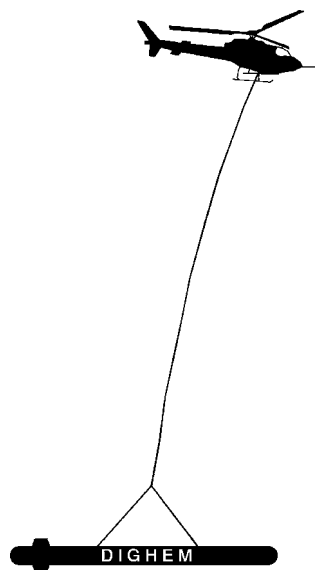Report #03091

# RESOLVE SURVEY
## FOR
## THE BRITISH COLUMBIA
## GEOLOGICAL SURVEY

## KOTCHO AREA, BC

Fugro Airborne Surveys Corp.
Mississauga, Ontario

Michael J. Cain
Geophysicist

January 2004

# SUMMARY

This report describes the logistics, data acquisition and processing of a RESOLVE airborne geophysical survey carried out for the British Columbia Geological Survey, over the Kotcho area, British Columbia. Total coverage of the survey blocks amounted to 252 km. The survey was flown from on November 23, 2003.

The purpose of the survey was to detect aggregate deposits. This was accomplished by using a RESOLVE multi-coil, multi-frequency electromagnetic system, supplemented by two high sensitivity cesium magnetometers in a horizontal gradiometer configuration. The information from these sensors was processed to produce maps that display the magnetic and conductive properties of the survey area. A GPS electronic navigation system ensured accurate positioning of the geophysical data with respect to the base maps.

The survey data were processed and compiled in the Fugro Airborne Surveys Toronto office. Map products and digital data were provided in accordance with the scales and formats specified in the Survey Agreement.

# CONTENTS

## APPENDICES

# 1. INTRODUCTION

A RESOLVE electromagnetic/resistivity/magnetic survey was flown for the British Columbia Geological Survey on November 23, 2003, over the Kotcho area, British Columbia.

Survey coverage consisted of 252 line-km, including 3 tie lines running 90° to the traverse lines. Flight lines were flown in an azimuthal direction of 346° with a line separation of 200 metres. A small detail area was flown with lines offset by 100 metres with respect to the main block giving an effective line spacing of 100 metres within the detail area.

The survey employed the RESOLVE electromagnetic system. Ancillary equipment consisted of a horizontal magnetic gradiometer, radar, laser and barometric altimeters, video camera, analog and digital recorders, and an electronic navigation system. The instrumentation was installed in an AS350-BA turbine helicopter (Registration C-GJIX) that was provided by Questral Helicopters Ltd. The helicopter flew at an average airspeed of 135 km/h with an EM sensor height of approximately 35 metres.

Figure 1: Fugro Airborne Surveys RESOLVE EM bird with AS350-B3

## 2. SURVEY OPERATIONS

The base of operations for the survey was established at Rainbow Lake, Alberta.  The survey was flown from on November 23, 2003 over one survey block.  The survey area can be located on NTS map sheet 94I/15 (Figure 2).

Total survey coverage consisted of 252 line-km, including 22 line-km of tie-lines.

The survey specifications were as follows:

| Parameter | Specifications |
|---|---|
| Traverse line direction | 346°/166° |
| Traverse line spacing | 200 m |
| Tie line direction | 256°/76° |
| Tie line spacing | 2500 m |
| Sample interval | 10 Hz or 3.8 m at 135 km/hr |
| Aircraft mean terrain clearance | 62 m |
| EM sensor mean terrain clearance | 35 m |
| Mag sensor mean terrain clearance | 35 m |
| Average speed | 135 km/hr |
| Navigation (guidance) | ±5 m, Real-time GPS |
| Post-survey flight path | ±2 m, Differential GPS |

**LOCATION MAP**

120°30'W

59°00'N

N

White

Spruce

Datcin

Creek

Creek

Sahaho Creek

NTS: 94I/15

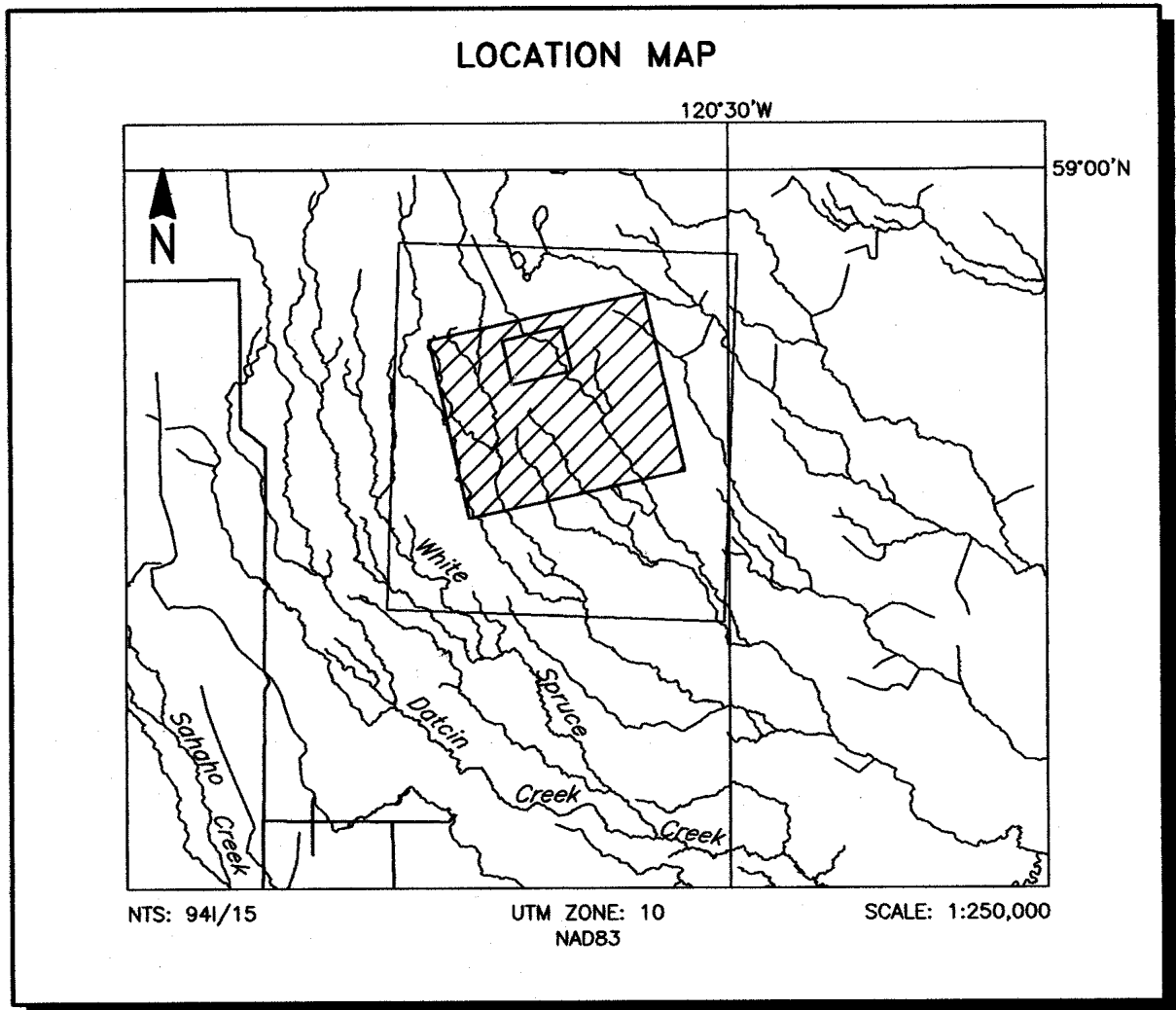UTM ZONE: 10
NAD83

SCALE: 1:250,000

Figure 2
Location Map and Sheet Layout
Kotcho Area
Job # 03091

# 3. SURVEY EQUIPMENT

This section provides a brief description of the geophysical instruments used to acquire the survey data and the calibration procedures employed. The geophysical equipment was installed in an AS350-BA helicopter. This aircraft provides a safe and efficient platform for surveys of this type.

## Electromagnetic System

Model: RESOLVE

Type: Towed bird, symmetric dipole configuration operated at a nominal survey altitude of 30 metres. Coil separation is 7.9 metres for 400 Hz, 1500 Hz, 6400 Hz, 25,000 Hz and 115,000 Hz coplanar coil-pairs; and 9.0 metres for the 3300 Hz coaxial coil-pair.

Coil orientations/frequencies:

| orientation | nominal | actual |
|---|---|---|
| coplanar | 400 Hz | 389 Hz |
| coplanar | 1500 Hz | 1574 Hz |
| coaxial | 3300 Hz | 3245 Hz |
| coplanar | 6400 Hz | 6075 Hz |
| coplanar | 25,000 Hz | 25,300 Hz |
| coplanar | 115,000 Hz | 114,940 Hz |

Channels recorded:
6 in-phase channels
6 quadrature channels
2 monitor channels

Sensitivity:
0.12 ppm at 400 Hz CP
0.12 ppm at 1500 Hz CP
0.12 ppm at 3300 Hz CX
0.24 ppm at 6400 Hz CP
0.60 ppm at 25,000 Hz CP
0.60 ppm at 115,000 Hz CP

Sample rate:
10 per second, equivalent to 1 sample every 3.8 m, at a survey speed of 135 km/h.

The electromagnetic system utilizes a multi-coil coaxial/coplanar technique to energize conductors in different directions.  The coaxial coils are vertical with their axes in the flight direction.   The coplanar coils are horizontal.   The secondary fields are sensed simultaneously by means of receiver coils that are maximum coupled to their respective transmitter coils.   The system yields an in-phase and a quadrature channel from each transmitter-receiver coil-pair.

## RESOLVE System Calibration

Calibration of the system during the survey uses the Fugro AutoCal automatic, internal calibration process.  At the beginning and end of each flight, and at intervals during the flight, the system is flown up to high altitude to remove it from any "ground effect" (response from the earth).  Any remaining signal from the receiver coils (base level) is measured as the zero level, and removed from the data collected until the time of the next calibration.  Following the zero level setting, internal calibration coils, for which the response phase and amplitude have been determined at the factory, are automatically triggered – one for each frequency.  The on-time of the coils is sufficient to determine an accurate response through any ambient noise.   The receiver response to each calibration coil "event" is compared to the expected response (from the factory calibration) for both phase angle and amplitude, and the applied phase and gain corrections are adjusted to bring the data to the correct value.  In addition, the output of the transmitter coils are continuously monitored during the survey, and the applied gains adjusted to correct for any change in transmitter output.

Because the internal calibration coils are calibrated at the factory (on a resistive halfspace) ground calibrations using external calibration coils on-site are not necessary for system calibration. A check calibration may be carried out on-site to ensure all systems are working correctly. All system calibrations will be carried out in the air, at sufficient altitude that there will be no measurable response from the ground.

The internal calibration coils are rigidly positioned and mounted in the system relative to the transmitter and receiver coils. In addition, when the internal calibration coils are calibrated at the factory, a rigid jig is employed to ensure accurate response from the external coils.

Using real time Fast Fourier Transforms and the calibration procedures outlined above, the data will be processed in real time from measured total field at a high sampling rate to in-phase and quadrature values at 10 samples per second.

## Airborne Magnetometer

Configuration:            Horizontal Gradiometer

Model:                    Fugro AM102 processor with two Scintrex CS2 sensors

Type:                     Optically pumped cesium vapour

Sensitivity:              0.01 nT

Sample rate:              10 per second

The horizontal gradiometer consists of two high sensitivity cesium sensors housed in a transverse mounted rigid boom at the rear of the HEM bird.  The sensor separation is 5 m and is flown 27 m below the helicopter.

## Magnetic Base Station

<u>Primary</u>

Model:                    Fugro CF1 base station with timing provided by integrated GPS

Sensor type:              Geometrics G822

Counter specifications:   Accuracy:      ±0.1 nT
                          Resolution:    0.01 nT
                          Sample rate    1 Hz

GPS specifications:       Model:         Marconi Allstar
                          Type:          Code and carrier tracking of L1 band,
                                         12-channel, C/A code at 1575.42 MHz
                          Sensitivity:   -90 dBm, 1.0 second update
                          Accuracy:      Manufacturer's stated accuracy for differential
                                         corrected GPS is 2 metres

Environmental
Monitor specifications:   Temperature:
- Accuracy:      ±1.5ºC max
- Resolution:    0.0305ºC
- Sample rate:  1 Hz
- Range:           -40ºC to +75ºC

Barometric pressure:
- Model:           Motorola MPXA4115A
- Accuracy:      ±3.0º kPa max (-20ºC to 105ºC temp. ranges)
- Resolution:    0.013 kPa
- Sample rate:  1 Hz
- Range:           55 kPa to 108 kPa

<u>Backup Magnetometer</u>

Model:                     GEM Systems GSM-19T

Type:                      Digital recording proton precession

Sensitivity:             0.10 nT

Sample rate:          3 second intervals

A digital recorder is operated in conjunction with the base station magnetometer to record the diurnal variations of the earth's magnetic field.  The clock of the base station is synchronized with that of the airborne system, using GPS time, to permit subsequent removal of diurnal drift.

# Navigation (Global Positioning System)

<u>Airborne Receiver for Real-time Navigation & Guidance</u>

Model:                   Ashtech Glonass GG24 with PNAV 2100 interface

Type:                    SPS (L1 band), 24-channel, C/A code at 1575.42 MHz,
                         S code at 0.5625 MHz, Real-time differential.

Sensitivity:             -132 dBm, 0.5 second update

Accuracy:                Manufacturer's stated accuracy is better than 5 metres
                         real-time

The antenna for the GPS guidance system is mounted on the tail fin of the helicopter.


<u>Airborne Receiver for Flight Path Recovery</u>

Model:                   Ashtech Dual Frequency Z-Surveyor

Type:                    Code and carrier tracking of L1 band, 12-channel, dual
                         frequency C/A code at 1575.2 MHz, and L2 P-code
                         1227 MHz

Sensitivity:             0.5 second update

Accuracy:                Manufacturer's stated accuracy for differential corrected
                         GPS is better than 1 metre


The antenna for the GPS flight path recovery system is housed on the rear of the EM bird.


<u>Primary Base Station for Post-Survey Differential Correction</u>

Model:                   Ashtech Dual Frequency Z-Surveyor

Type:                    Code and carrier tracking of L1 band, 12-channel, dual
                         frequency C/A code at 1575.2 MHz, and L2 P-code
                         1227 MHz

Sensitivity:             1.0 second update

Accuracy:                Manufacturer's stated accuracy for differential corrected
                         GPS is better than 1 metre

Secondary GPS Base Station

| | |
|---|---|
| Model: | Marconi Allstar OEM, CMT-1200 |
| Type: | Code and carrier tracking of L1 band, 12-channel, C/A code at 1575.42 MHz |
| Sensitivity: | -90 dBm, 1.0 second update |
| Accuracy: | Manufacturer's stated accuracy for differential corrected GPS is 2 metres. |

The Ashtech GG24 is a line of sight, satellite navigation system that utilizes time-coded signals from at least four of forty-eight available satellites. Both Russian GLONASS and American NAVSTAR satellite constellations are used to calculate the position and to provide real time guidance to the helicopter. For flight path processing an Ashtech Z-surveyor was used as the mobile receiver. A similar system was used as the primary base station receiver. The mobile and base station raw XYZ data were recorded, thereby permitting post-survey differential corrections for theoretical accuracies of better than 2 metres. A Marconi Allstar GPS unit was used as a secondary (back-up) base station.

Although the base station receiver is able to calculate its own latitude and longitude, a higher degree of accuracy can be obtained if the reference unit is established on a known benchmark or triangulation point. For this survey, the primary GPS station was located at latitude 58° 29' 38.3184", longitude -119° 24' 55.0227" and an elevation of 521.3 metres above the ellipsoid. The GPS records data relative to the WGS84 ellipsoid, which is the basis of the revised North American Datum (NAD83).

## Radar Altimeter

| | |
|---|---|
| Manufacturer: | Honeywell/Sperry |
| Model: | RT330 |
| Type: | Short pulse modulation, 4.3 GHz |
| Sensitivity: | 0.3 m |

The radar altimeter measures the vertical distance between the helicopter and the ground. This information is used in the processing algorithm that determines conductor depth.

## Barometric Pressure and Temperature Sensors

| | | |
|---|---|---|
| Model: | DIGHEM D 1300 | |
| Type: | Motorola MPX4115AP analog pressure sensor | |
| | AD592AN high-impedance remote temperature sensors | |
| Sensitivity: | Pressure: | 150 mV/kPa |
| | Temperature: | 100 mV/°C or 10 mV/°C (selectable) |
| Sample rate: | 10 per second | |

The D1300 circuit is used in conjunction with one barometric sensor and up to three temperature sensors. Two sensors (baro and temp) are installed in the EM console in the aircraft, to monitor pressure and internal operating temperatures.

## Laser Altimeter

| | |
|---|---|
| Manufacturer: | Optech |
| Model: | G150 |

Type:     Fixed pulse repetition rate of 2 kHz

Sensitivity:    ±5 cm from 10ºC to 30ºC
       ±10 cm from -20ºC to +50ºC

The laser altimeter is housed in the EM bird, and measures the distance from the EM bird to ground, except in areas of dense tree cover.

## Analog Recorder

Manufacturer:   RMS Instruments

Type:     DGR33 dot-matrix graphics recorder

Resolution:    4x4 dots/mm

Speed:     1.5 mm/sec

The analog profiles are recorded on chart paper in the aircraft during the survey.  Table 3-1 lists the geophysical data channels and the vertical scale of each profile.

## Digital Data Acquisition System

Manufacturer:   RMS Instruments

Model:     DGR 33

Recorder:    San Disk compact flash card (PCMCIA)

The data are stored on flash cards and are downloaded to the field workstation PC at the survey base for verification, backup and preparation of in-field products.

# Flight Path Video Recording System

Recorder:              Panasonic AG-720

Fiducial numbers are recorded continuously and are displayed on the margin of each image.  This procedure ensures accurate correlation of analog and digital data with respect to visible features on the ground.

## Table 3-1.  The Analog Profiles

| Channel Name | Parameter | Scale units/mm |
|---|---|---|
| 400I | coaxial in-phase        (        400 Hz) | 5 ppm |
| 400Q | coaxial quad             (        400 Hz) | 5 ppm |
| 1K5I | coplanar in-phase     (     1500 Hz) | 5 ppm |
| 1K5Q | coplanar quad          (     1500 Hz) | 5 ppm |
| 1X8I | coaxial in-phase        (     3300 Hz) | 5 ppm |
| 1X8Q | coaxial quad             (     3300 Hz) | 5 ppm |
| 6K2I | coplanar in-phase     (     6200 Hz) | 10 ppm |
| 6K2Q | coplanar quad          (     6200 Hz) | 10 ppm |
| 25KI | coplanar in-phase     (  25,000 Hz) | 40 ppm |
| 25KQ | coplanar quad          (  25,000 Hz) | 40 ppm |
| 100I | coplanar inphase     (115,000 Hz) | 40 ppm |
| 100Q | coplanar quad         (115,000 Hz) | 40 ppm |
| ALTL | altimeter (laser) | 3 m |
| ALTR | altimeter (radar) | 3 m |
| MAG1 | magnetics, coarse | 20 nT |
| 1SP | coaxial spherics monitor | |
| 2SP | coplanar spherics monitor | |
| 2PL | coplanar powerline monitor | |
| 1KPA | altimeter (barometric) | 30 m |
| 2TDC | internal (console) temperature | 1° C |
| 3TDC | external temperature | 1° C |

# 4. QUALITY CONTROL AND IN-FIELD PROCESSING

Digital data for each flight were transferred to the field workstation, in order to verify data quality and completeness. A database was created and updated using Geosoft Oasis Montaj and proprietary Fugro Atlas software. This allowed the field personnel to calculate, display and verify both the positional (flight path) and geophysical data on a screen or printer. Analog records were examined as a preliminary assessment of the data acquired for each flight.

In-field processing of Fugro survey data consists of differential corrections to the airborne GPS data, verification of EM calibrations, drift correction of the raw airborne EM data, spike rejection and filtering of all geophysical and ancillary data, verification of flight videos, calculation of preliminary resistivity data, diurnal correction, and preliminary leveling of magnetic data.

All data, including base station records, were checked on a daily basis, to ensure compliance with the survey contract specifications. Reflights were required if any of the standard specifications were not met.

## 5. DATA PROCESSING

### Flight Path Recovery

The raw range data from at least four satellites are simultaneously recorded by both the base and mobile GPS units. The geographic positions of both units, relative to the model ellipsoid, are calculated from this information. Differential corrections, which are obtained from the base station, are applied to the mobile unit data to provide a post-flight track of the aircraft, accurate to within 2 m. Speed checks of the flight path are also carried out to determine if there are any spikes or gaps in the data.

The corrected WGS84 latitude/longitude coordinates are transformed to the coordinate system used on the final maps. Images or plots are then created to provide a visual check of the flight path.

### Electromagnetic Data/Apparent Resistivity

EM data are processed at the recorded sample rate of 10 samples/second. Spheric rejection median and Hanning filters were applied to reduce noise to acceptable levels.

The apparent resistivity in ohm-m were generated from the in-phase and quadrature EM components for all of the coplanar frequencies, using a pseudo-layer half-space model. The inputs to the resistivity algorithm are the inphase and quadrature amplitudes of the secondary field. The algorithm calculates the apparent resistivity in ohm-m, and the apparent height of the bird above the conductive source. Any difference between the

apparent height and the true height, as measured by the radar altimeter, is called the pseudo-layer and reflects the difference between the real geology and a homogeneous halfspace. This difference is often attributed to the presence of a highly resistive upper layer. Any errors in the altimeter reading, caused by heavy tree cover, are included in the pseudo-layer and do not affect the resistivity calculation. The apparent depth estimates, however, will reflect the altimeter errors. Apparent resistivity calculated in this manner may behave quite differently from those calculated using other models.

In areas of high magnetic permeability or dielectric permittivity, the calculated resistivities will be erroneously high. Various algorithms and inversion techniques can be used to partially correct for this effect.

The preliminary apparent resistivity maps and images were carefully inspected to identify any lines or line segments that might require base level adjustments. Subtle changes between in-flight calibrations of the system can result in line-to-line differences that are more recognizable in resistive (low signal amplitude) areas. Manual leveling was carried out to eliminate or minimize resistivity differences that can be attributed, in part, to changes in operating temperatures. These leveling adjustments were usually very subtle, and do not result in the degradation of discrete anomalies.

After the manual leveling process is complete, the data were subjected to a microleveling technique in order to remove any remaining line-to-line differences within the calculated resistivities.

Apparent resistivity grids, which display the conductive properties of the survey areas, were produced from the 400 Hz, 1500 Hz, 6400 Hz, 25,000 Hz and 115,000 Hz coplanar data. The calculated resistivities for the five coplanar frequencies are included in the XYZ and grid archives.  Values are in ohm-metres on all final products.


## Total Magnetic Field

The aeromagnetic data were inspected in grid and profile format.  Spikes were removed manually with the aid of a fourth difference calculation.  A Geometrics G822 cesium vapour magnetometer was operated at the survey base to record diurnal variations of the earth's magnetic field.  The clock of the base station was synchronized with that of the airborne system to permit subsequent removal of diurnal drift.  The data were inspected for spikes and filtered.  The filtered diurnal data were subtracted from the total field magnetic data.  Grids of the diurnally corrected aeromagnetic data were created and contoured.  A lag correction was applied to the magnetic data.  The results were then leveled using tie and traverse line intercepts.  Manual adjustments were applied to any lines that required leveling, as indicated by shadowed images of both the total field magnetic data and the calculated vertical gradient data.  A microleveling algorithm was used to make any remaining subtle leveling adjustments.

## Contour, Colour and Shadow Map Displays

The geophysical data are interpolated onto a regular grid using a modified Akima spline technique. The resulting grid is suitable for image processing and generation of contour maps. The grid cell size was 40 metres or 20% of the line interval.

Colour maps are produced by interpolating the grid down to the pixel size. The parameter is then incremented with respect to specific amplitude ranges to provide colour "contour" maps.

Monochromatic shadow maps or images can be generated by employing an artificial sun to cast shadows on a surface defined by the geophysical grid. There are many variations in the shadowing technique. These techniques can be applied to total field or enhanced magnetic data, magnetic derivatives, resistivity, etc. The shadowing technique is also used as a quality control method to detect subtle changes between lines.

# 6. PRODUCTS

This section lists the final maps and products that have been provided under the terms of the survey agreement.  Other products can be prepared from the existing dataset, if requested.  These include magnetic enhancements or derivatives, percent magnetite, resistivities corrected for magnetic permeability and/or dielectric permittivity, digital terrain, resistivity-depth sections, inversions, and overburden thickness.

## Base Maps

Base maps of the survey area were produced by scanning published topographic maps to a bitmap (.bmp) format.  This process provides a relatively accurate, distortion free base that facilitates correlation of the navigation data to the map coordinate system. The topographic files were combined with geophysical data for plotting the final maps. All maps were created using the following parameters:

Projection Description:

| | |
|---|---|
| Datum: | NAD 83 |
| Ellipsoid: | WGS84 |
| Projection: | UTM (Zone:  10) |
| Central Meridian: | 123° West |
| False Northing: | 0 |
| False Easting: | 500000 |
| Scale Factor: | 0.9996 |

The following parameters are presented on 1 map sheet, at a scale of 1:20,000.  All maps include flight lines and topography.  Preliminary products are not listed.

## Final Products

<u>Colour Maps (2 copies) at 1:20000</u>

Total Magnetic Field maps
Apparent Resistivity 400 Hz
Apparent Resistivity 1500 Hz
Apparent Resistivity 6200 Hz
Apparent Resistivity 25,000 Hz
Apparent Resistivity 115,000 Hz

<u>Additional Products</u>

Digital Archive on CD-ROM                    2 copies
Survey Report                                3 copies
Analog Chart Records                         All flights
Flight Path Video (VHS)                      1 video cassette

## 7.  CONCLUSIONS AND RECOMMENDATIONS

This report provides a description of the equipment, data processing procedures and logistics of the survey.

The various maps included with this report display the magnetic and conductive properties of the survey area.  It is recommended that a complete assessment and detailed evaluation of the survey results be carried out, in conjunction with all available geophysical, geological and geochemical information.

It is also recommended that image processing of existing geophysical data be considered, in order to extract the maximum amount of information from the survey results.  Current software and imaging techniques often provide valuable information on structure and lithology, which may not be clearly evident on the contour and colour maps. These techniques can yield images that define subtle, but significant, structural details.

Respectfully submitted,

**FUGRO AIRBORNE SURVEYS CORP.**

Michael Cain
Geophysicist

# APPENDIX A
# LIST OF PERSONNEL

The following personnel were involved in the acquisition, processing, interpretation and presentation of data, relating to a RESOLVE airborne geophysical survey carried out for the British Columbia Geological Survey, over the Kotcho area, British Columbia

| | |
|---|---|
| David Miles | Manager, Helicopter Operations |
| Emily Farquhar | Manager, Data Processing and Interpretation |
| Michael Cain | Project Geophysicist |
| Will Marr | Geophysical Operator |
| Igor Sram | Field Geophysicist |
| Bill Hofstede | Pilot (Questral Helicopters Ltd.) |
| Lyn Vanderstarren | Drafting Supervisor |
| Albina Tonello | Secretary/Expeditor |

The survey consisted of 252 km of coverage, flown on November 23, 2003.

All personnel are employees of Fugro Airborne Surveys, except for the pilot who is an employee of Questral Helicopters Ltd.

# APPENDIX B
# OPTIONAL PRODUCTS


## Digital Terrain


The radar altimeter values (ALTR – aircraft to ground clearance) are subtracted from the differentially corrected and de-spiked GPS-Z values to produce profiles of the height above the ellipsoid along the survey lines.  These values are gridded to produce contour maps showing approximate elevations within the survey area.  The calculated digital terrain data are then tie-line leveled and adjusted to mean sea level.  Any remaining subtle line-to-line discrepancies are manually removed.  After the manual corrections are applied, the digital terrain data are filtered with a microleveling algorithm.


The accuracy of the elevation calculation is directly dependent on the accuracy of the two input parameters, ALTR and GPS-Z.  The ALTR value may be erroneous in areas of heavy tree cover, where the altimeter reflects the distance to the tree canopy rather than the ground.  The GPS-Z value is primarily dependent on the number of available satellites.  Although post-processing of GPS data will yield X and Y accuracies in the order of 1-2 metres, the accuracy of the Z value is usually much less, sometimes in the ±10 metre range.  Further inaccuracies may be introduced during the interpolation and gridding process.


Because of the inherent inaccuracies of this method, no guarantee is made or implied that the information displayed is a true representation of the height above sea level.  Although this product may be of some use as a general reference, THIS PRODUCT MUST NOT BE USED FOR NAVIGATION PURPOSES.

## Dielectric Permittivity and Magnetic Permeability Corrections[1]

In resistive areas having magnetic rocks, the magnetic and dielectric effects will both generally be present in high-frequency EM data, whereas only the magnetic effect will exist in low-frequency data.

The magnetic permeability is first obtained from the EM data at the lowest frequency (385 Hz) because the ratio of the magnetic response to conductive response is maximized and because displacement currents are negligible.  The homogeneous half-space model is used.  The computed magnetic permeability is then used along with the inphase and quadrature response at the highest frequency to obtain the relative dielectric permittivity, again using the homogeneous half-space model.  The highest frequency is used because the ratio of dielectric response to conductive response is maximized.  The resistivity can then be determined from the measured inphase and quadrature components of each frequency, given the relative magnetic permeability and relative dielectric permittivity.

## Horizontal Gradient Enhanced Total Magnetic Field

Bidirectional gridding with the cross-line gradient should produce a surface that correctly renders both the measured data and the measured horizontal gradient at each survey

line.  This can be an advantage when gridding data that include features approaching the line separation in size and also for rendering features that are not perpendicular to the line direction, particularly those which are sub-parallel to the line direction.  Direct results of the application of Horizontal Gradient Enhanced (HGE) gridding are:

- Increased resolution and continuity of magnetic features parallel or sub-parallel to the flight line direction.

- Correct spatial positioning of finite source magnetic bodies between lines.

- Improved resolution of analytical signal and enhanced analytic signal products.

## Calculated Vertical Magnetic Gradient

The horizontal gradient enhanced total magnetic field data were subjected to a processing algorithm that enhances the response of magnetic bodies in the upper 500 m and attenuates the response of deeper bodies.  The resulting vertical gradient map provides better definition and resolution of near-surface magnetic units.  It also identifies weak magnetic features that may not be evident on the total field map.  However, regional magnetic variations and changes in lithology may be better defined on the total magnetic field map.

## Multi-channel Stacked Profiles

Distance-based profiles of the digitally recorded geophysical data can be generated and plotted at an appropriate scale.  These profiles also contain the calculated parameters that

[1] Huang, H. and Fraser, D.C., 2001 Mapping of the Resistivity, Susceptibility, and Permittivity of

are used in the interpretation process. These are produced as worksheets prior to interpretation, and are also presented in the final corrected form after interpretation.

## Resistivity-depth Sections

The apparent resistivities for all frequencies can be displayed simultaneously as coloured resistivity-depth sections. Usually, only the coplanar data are displayed as the close frequency separation between the coplanar and adjacent coaxial data tends to distort the section. The sections can be plotted using the topographic elevation profile as the surface. The digital terrain values, in metres a.m.s.l., can be calculated from the GPS Z-value or barometric altimeter, minus the aircraft radar altimeter.

Resistivity-depth sections can be generated in three formats:

(1)     Sengpiel resistivity sections, where the apparent resistivity for each frequency is plotted at the depth of the centroid of the in-phase current flow[2]; and,

(2)     Differential resistivity sections, where the differential resistivity is plotted at the differential depth[3].

(3)     Occam[4] or Multi-layer[5] inversion.

---

the Earth Using a Helicopter-borne Electromagnetic System: Geophysics 106 pg 148-157.

[2]     Sengpiel, K.P., 1988, Approximate Inversion of Airborne EM Data from Multilayered Ground: Geophysical Prospecting 36, 446-459.

[3]     Huang, H. and Fraser, D.C., 1993, Differential Resistivity Method for Multi-frequency Airborne EM Sounding: presented at Intern. Airb. EM Workshop, Tucson, Ariz.

[4]     Constable et al, 1987, Occam's inversion: a practical algorithm for generating smooth models from electromagnetic sounding data: Geophysics, 52, 289-300.

[5]     Huang H., and Palacky, G.J., 1991, Damped least-squares inversion of time domain airborne EM data based on singular value decomposition: Geophysical Prospecting, 39, 827-844.

Both the Sengpiel and differential methods are derived from the pseudo-layer half-space model.  Both yield a coloured resistivity-depth section that attempts to portray a smoothed approximation of the true resistivity distribution with depth.  Resistivity-depth sections are most useful in conductive layered situations, but may be unreliable in areas of moderate to high resistivity where signal amplitudes are weak.  In areas where in-phase responses have been suppressed by the effects of magnetite, or adversely affected by cultural features, the computed resistivities shown on the sections may be unreliable.

Both the Occam and multi-layer inversions compute the layered earth resistivity model that would best match the measured EM data.  The Occam inversion uses a series of thin, fixed layers (usually 20 x 5m and 10 x 10m layers) and computes resistivities to fit the EM data.  The multi-layer inversion computes the resistivity and thickness for each of a defined number of layers (typically 3-5 layers) to best fit the data.

## EM Magnetite

The apparent percent magnetite by weight is computed wherever magnetite produces a negative in-phase EM response.  This calculation is more meaningful in resistive areas.

## Magnetic Derivatives

The total magnetic field data can be subjected to a variety of filtering techniques to yield maps or images of the following:

enhanced magnetics

second vertical derivative

reduction to the pole/equator

magnetic susceptibility with reduction to the pole

upward/downward continuations

analytic signal

All of these filtering techniques improve the recognition of near-surface magnetic bodies, with the exception of upward continuation. Any of these parameters can be produced on request.

# APPENDIX C
# BACKGROUND INFORMATION

## Electromagnetics

Fugro electromagnetic responses fall into two general classes, discrete and broad. The discrete class consists of sharp, well-defined anomalies from discrete conductors such as sulphide lenses and steeply dipping sheets of graphite and sulphides. The broad class consists of wide anomalies from conductors having a large horizontal surface such as flatly dipping graphite or sulphide sheets, saline water-saturated sedimentary formations, conductive overburden and rock, kimberlite pipes and geothermal zones. A vertical conductive slab with a width of 200 m would straddle these two classes.

The vertical sheet (half plane) is the most common model used for the analysis of discrete conductors. All anomalies plotted on the geophysical maps are analyzed according to this model. The following section entitled **Discrete Conductor Analysis** describes this model in detail, including the effect of using it on anomalies caused by broad conductors such as conductive overburden.
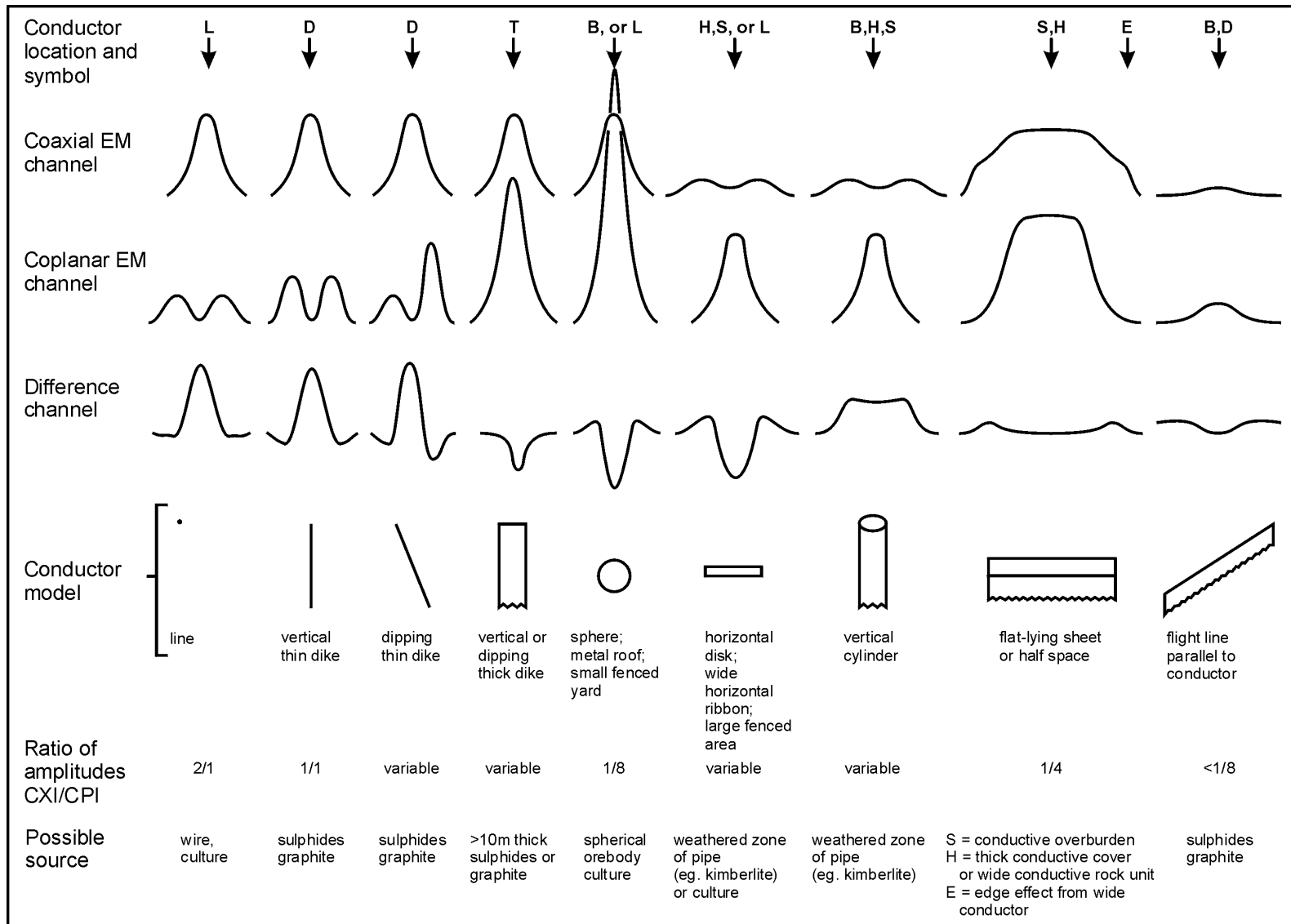
The conductive earth (half-space) model is suitable for broad conductors. Resistivity contour maps result from the use of this model. A later section entitled **Resistivity Mapping** describes the method further, including the effect of using it on anomalies caused by discrete conductors such as sulphide bodies.

## Geometric Interpretation

The geophysical interpreter attempts to determine the geometric shape and dip of the conductor. Figure C-1 shows typical HEM anomaly shapes which are used to guide the geometric interpretation.

## Discrete Conductor Analysis

The EM anomalies appearing on the electromagnetic map are analyzed by computer to give the conductance (i.e., conductivity-thickness product) in siemens (mhos) of a vertical sheet model. This is done regardless of the interpreted geometric shape of the conductor. This is not an unreasonable procedure, because the computed conductance increases as the electrical quality of the conductor increases, regardless of its true shape. DIGHEM anomalies are divided into seven grades of conductance, as shown in Table C-1. The conductance in siemens (mhos) is the reciprocal of resistance in ohms.

| Conductor location and symbol | L | D | D | T | B, or L | H,S, or L | B,H,S | S,H | E | B,D |
|---|---|---|---|---|---|---|---|---|---|---|
| Coaxial EM channel | | | | | | | | | | |
| Coplanar EM channel | | | | | | | | | | |
| Difference channel | | | | | | | | | | |
| Conductor model | line | vertical thin dike | dipping thin dike | vertical or dipping thick dike | sphere; metal roof; small fenced yard | horizontal disk; wide horizontal ribbon; large fenced area | vertical cylinder | flat-lying sheet or half space | | flight line parallel to conductor |
| Ratio of amplitudes CXI/CPI | 2/1 | 1/1 | variable | variable | 1/8 | variable | variable | 1/4 | | <1/8 |
| Possible source | wire, culture | sulphides graphite | sulphides graphite | >10m thick sulphides or graphite | spherical orebody culture | weathered zone of pipe (eg. kimberlite) or culture | weathered zone of pipe (eg. kimberlite) | S = conductive overburden<br>H = thick conductive cover or wide conductive rock unit<br>E = edge effect from wide conductor | | sulphides graphite |

**Typical DIGHEM anomaly shapes**

**Figure C-1**

The conductance value is a geological parameter because it is a characteristic of the conductor alone.  It generally is independent of frequency, flying height or depth of burial, apart from the averaging over a greater portion of the conductor as height increases.  Small anomalies from deeply buried strong conductors are not confused with small anomalies from shallow weak conductors because the former will have larger conductance values.

## Table C-1.  EM Anomaly Grades

| Anomaly Grade | Siemens |
|:---:|:---:|
| 7 | > 100 |
| 6 | 50  –  100 |
| 5 | 20  –   50 |
| 4 | 10  –   20 |
| 3 | 5  –   10 |
| 2 | 1  –    5 |
| 1 | <    1 |

Conductive overburden generally produces broad EM responses which may not be shown as anomalies on the geophysical maps.   However, patchy conductive overburden in otherwise resistive areas can yield discrete anomalies with a conductance grade (cf. Table C-1) of 1, 2 or even 3 for conducting clays which have resistivities as low as 50 ohm-m. In areas where ground resistivities are below 10 ohm-m, anomalies caused by weathering variations and similar causes can have any conductance grade.  The anomaly shapes from the multiple coils often allow such conductors to be recognized, and these are indicated by the letters S, H, and sometimes E on the geophysical maps (see EM legend on maps).

For bedrock conductors, the higher anomaly grades indicate increasingly higher conductances.  Examples:  the New Insco copper discovery (Noranda, Canada) yielded a grade 5 anomaly, as did the neighbouring copper-zinc Magusi River ore body; Mattabi (copper-zinc, Sturgeon Lake, Canada) and Whistle (nickel, Sudbury, Canada) gave grade 6; and the Montcalm nickel-copper discovery (Timmins, Canada) yielded a grade 7 anomaly. Graphite and sulphides can span all grades but, in any particular survey area, field work may show that the different grades indicate different types of conductors.

Strong conductors (i.e., grades 6 and 7) are characteristic of massive sulphides or graphite.  Moderate conductors (grades 4 and 5) typically reflect graphite or sulphides of a less massive character, while weak bedrock conductors (grades 1 to 3) can signify poorly connected graphite or heavily disseminated sulphides.  Grades 1 and 2 conductors may not respond to ground EM equipment using frequencies less than 2000 Hz.

The presence of sphalerite or gangue can result in ore deposits having weak to moderate conductances.   As an example, the three million ton lead-zinc deposit of Restigouche Mining Corporation near Bathurst, Canada, yielded a well-defined grade 2 conductor.  The 10 percent by volume of sphalerite occurs as a coating around the fine grained massive pyrite, thereby inhibiting electrical conduction. Faults, fractures and shear zones may produce anomalies that typically have low conductances (e.g., grades 1 to 3).  Conductive rock formations can yield anomalies of any conductance grade.  The conductive materials in

such rock formations can be salt water, weathered products such as clays, original depositional clays, and carbonaceous material.

For each interpreted electromagnetic anomaly on the geophysical maps, a letter identifier and an interpretive symbol are plotted beside the EM grade symbol. The horizontal rows of dots, under the interpretive symbol, indicate the anomaly amplitude on the flight record. The vertical column of dots, under the anomaly letter, gives the estimated depth. In areas where anomalies are crowded, the letter identifiers, interpretive symbols and dots may be obliterated. The EM grade symbols, however, will always be discernible, and the obliterated information can be obtained from the anomaly listing appended to this report.

The purpose of indicating the anomaly amplitude by dots is to provide an estimate of the reliability of the conductance calculation. Thus, a conductance value obtained from a large ppm anomaly (3 or 4 dots) will tend to be accurate whereas one obtained from a small ppm anomaly (no dots) could be quite inaccurate. The absence of amplitude dots indicates that the anomaly from the coaxial coil-pair is 5 ppm or less on both the in-phase and quadrature channels. Such small anomalies could reflect a weak conductor at the surface or a stronger conductor at depth. The conductance grade and depth estimate illustrates which of these possibilities fits the recorded data best.

The conductance measurement is considered more reliable than the depth estimate. There are a number of factors that can produce an error in the depth estimate, including the averaging of topographic variations by the altimeter, overlying conductive overburden, and the location and attitude of the conductor relative to the flight line. Conductor location and attitude can provide an erroneous depth estimate because the stronger part of the conductor may be deeper or to one side of the flight line, or because it has a shallow dip. A heavy tree cover can also produce errors in depth estimates. This is because the depth estimate is computed as the distance of bird from conductor, minus the altimeter reading. The altimeter can lock onto the top of a dense forest canopy. This situation yields an erroneously large depth estimate but does not affect the conductance estimate.

Dip symbols are used to indicate the direction of dip of conductors. These symbols are used only when the anomaly shapes are unambiguous, which usually requires a fairly resistive environment.

A further interpretation is presented on the EM map by means of the line-to-line correlation of bedrock anomalies, which is based on a comparison of anomaly shapes on adjacent lines. This provides conductor axes that may define the geological structure over portions of the survey area. The absence of conductor axes in an area implies that anomalies could not be correlated from line to line with reasonable confidence.

The electromagnetic anomalies are designed to provide a correct impression of conductor quality by means of the conductance grade symbols. The symbols can stand alone with geology when planning a follow-up program. The actual conductance values are printed in the attached anomaly list for those who wish quantitative data. The anomaly ppm and depth are indicated by inconspicuous dots which should not distract from the conductor patterns, while being helpful to those who wish this information. The map provides an

interpretation of conductors in terms of length, strike and dip, geometric shape, conductance, depth, and thickness. The accuracy is comparable to an interpretation from a high quality ground EM survey having the same line spacing.

The appended EM anomaly list provides a tabulation of anomalies in ppm, conductance, and depth for the vertical sheet model. No conductance or depth estimates are shown for weak anomalous responses that are not of sufficient amplitude to yield reliable calculations.

Since discrete bodies normally are the targets of EM surveys, local base (or zero) levels are used to compute local anomaly amplitudes. This contrasts with the use of true zero levels which are used to compute true EM amplitudes. Local anomaly amplitudes are shown in the EM anomaly list and these are used to compute the vertical sheet parameters of conductance and depth.

## Questionable Anomalies

The EM maps may contain anomalous responses that are displayed as asterisks (*). These responses denote weak anomalies of indeterminate conductance, which may reflect one of the following: a weak conductor near the surface, a strong conductor at depth (e.g., 100 to 120 m below surface) or to one side of the flight line, or aerodynamic noise. Those responses that have the appearance of valid bedrock anomalies on the flight profiles are indicated by appropriate interpretive symbols (see EM legend on maps). The others probably do not warrant further investigation unless their locations are of considerable geological interest.

## The Thickness Parameter

A comparison of coaxial and coplanar shapes can provide an indication of the thickness of a steeply dipping conductor. The amplitude of the coplanar anomaly (e.g., CPI channel) increases relative to the coaxial anomaly (e.g., CXI) as the apparent thickness increases, i.e., the thickness in the horizontal plane. (The thickness is equal to the conductor width if the conductor dips at 90 degrees and strikes at right angles to the flight line.) This report refers to a conductor as <u>thin</u> when the thickness is likely to be less than 3 m, and <u>thick</u> when in excess of 10 m. Thick conductors are indicated on the EM map by parentheses "( )". For base metal exploration in steeply dipping geology, thick conductors can be high priority targets because many massive sulphide ore bodies are thick. The system cannot sense the thickness when the strike of the conductor is subparallel to the flight line, when the conductor has a shallow dip, when the anomaly amplitudes are small, or when the resistivity of the environment is below 100 ohm-m.

## Resistivity Mapping

Resistivity mapping is useful in areas where broad or flat lying conductive units are of interest. One example of this is the clay alteration which is associated with Carlin-type

deposits in the south west United States. The resistivity parameter was able to identify the clay alteration zone over the Cove deposit. The alteration zone appeared as a strong resistivity low on the 900 Hz resistivity parameter. The 7,200 Hz and 56,000 Hz resistivities showed more detail in the covering sediments, and delineated a range front fault. This is typical in many areas of the south west United States, where conductive near surface sediments, which may sometimes be alkalic, attenuate the higher frequencies.

Resistivity mapping has proven successful for locating diatremes in diamond exploration. Weathering products from relatively soft kimberlite pipes produce a resistivity contrast with the unaltered host rock. In many cases weathered kimberlite pipes were associated with thick conductive layers that contrasted with overlying or adjacent relatively thin layers of lake bottom sediments or overburden.

Areas of widespread conductivity are commonly encountered during surveys. These conductive zones may reflect alteration zones, shallow-dipping sulphide or graphite-rich units, saline ground water, or conductive overburden. In such areas, EM amplitude changes can be generated by decreases of only 5 m in survey altitude, as well as by increases in conductivity. The typical flight record in conductive areas is characterized by in-phase and quadrature channels that are continuously active. Local EM peaks reflect either increases in conductivity of the earth or decreases in survey altitude. For such conductive areas, apparent resistivity profiles and contour maps are necessary for the correct interpretation of the airborne data. The advantage of the resistivity parameter is that anomalies caused by altitude changes are virtually eliminated, so the resistivity data reflect only those anomalies caused by conductivity changes. The resistivity analysis also helps the interpreter to differentiate between conductive bedrock and conductive overburden. For example, discrete conductors will generally appear as narrow lows on the contour map and broad conductors (e.g., overburden) will appear as wide lows.

The apparent resistivity is calculated using the pseudo-layer (or buried) half-space model defined by Fraser (1978)[6]. This model consists of a resistive layer overlying a conductive half-space. The depth channels give the apparent depth below surface of the conductive material. The apparent depth is simply the apparent thickness of the overlying resistive layer. The apparent depth (or thickness) parameter will be positive when the upper layer is more resistive than the underlying material, in which case the apparent depth may be quite close to the true depth.

The apparent depth will be negative when the upper layer is more conductive than the underlying material, and will be zero when a homogeneous half-space exists. The apparent depth parameter must be interpreted cautiously because it will contain any errors that might exist in the measured altitude of the EM bird (e.g., as caused by a dense tree cover). The inputs to the resistivity algorithm are the in-phase and quadrature components of the coplanar coil-pair. The outputs are the apparent resistivity of the conductive half-space (the

[6]     Resistivity mapping with an airborne multicoil electromagnetic system:  Geophysics, v. 43, p.144-172

source) and the sensor-source distance. The flying height is not an input variable, and the output resistivity and sensor-source distance are independent of the flying height when the conductivity of the measured material is sufficient to yield significant in-phase as well as quadrature responses. The apparent depth, discussed above, is simply the sensor-source distance minus the measured altitude or flying height. Consequently, errors in the measured altitude will affect the apparent depth parameter but not the apparent resistivity parameter.

The apparent depth parameter is a useful indicator of simple layering in areas lacking a heavy tree cover. Depth information has been used for permafrost mapping, where positive apparent depths were used as a measure of permafrost thickness. However, little quantitative use has been made of negative apparent depths because the absolute value of the negative depth is not a measure of the thickness of the conductive upper layer and, therefore, is not meaningful physically. Qualitatively, a negative apparent depth estimate usually shows that the EM anomaly is caused by conductive overburden. Consequently, the apparent depth channel can be of significant help in distinguishing between overburden and bedrock conductors.

## Interpretation in Conductive Environments

Environments having low background resistivities (e.g., below 30 ohm-m for a 900 Hz system) yield very large responses from the conductive ground. This usually prohibits the recognition of discrete bedrock conductors. However, Fugro data processing techniques produce three parameters that contribute significantly to the recognition of bedrock conductors in conductive environments. These are the in-phase and quadrature difference channels (DIFI and DIFQ, which are available only on systems with "common" frequencies on orthogonal coil pairs), and the resistivity and depth channels (RES and DEP) for each coplanar frequency.

The EM difference channels (DIFI and DIFQ) eliminate most of the responses from conductive ground, leaving responses from bedrock conductors, cultural features (e.g., telephone lines, fences, etc.) and edge effects. Edge effects often occur near the perimeter of broad conductive zones. This can be a source of geologic noise. While edge effects yield anomalies on the EM difference channels, they do not produce resistivity anomalies. Consequently, the resistivity channel aids in eliminating anomalies due to edge effects. On the other hand, resistivity anomalies will coincide with the most highly conductive sections of conductive ground, and this is another source of geologic noise. The recognition of a bedrock conductor in a conductive environment therefore is based on the anomalous responses of the two difference channels (DIFI and DIFQ) and the resistivity channels (RES). The most favourable situation is where anomalies coincide on all channels.

The DEP channels, which give the apparent depth to the conductive material, also help to determine whether a conductive response arises from surficial material or from a conductive zone in the bedrock. When these channels ride above the zero level on the depth profiles (i.e., depth is negative), it implies that the EM and resistivity profiles are responding primarily to a conductive upper layer, i.e., conductive overburden. If the DEP channels are below the zero level, it indicates that a resistive upper layer exists, and this usually implies the

existence of a bedrock conductor.  If the low frequency DEP channel is below the zero level and the high frequency DEP is above, this suggests that a bedrock conductor occurs beneath conductive cover.

## Reduction of Geologic Noise

Geologic noise refers to unwanted geophysical responses.  For purposes of airborne EM surveying, geologic noise refers to EM responses caused by conductive overburden and magnetic permeability.  It was mentioned previously that the EM difference channels (i.e., channel DIFI for in-phase and DIFQ for quadrature) tend to eliminate the response of conductive overburden.

Magnetite produces a form of geological noise on the in-phase channels.  Rocks containing less than 1% magnetite can yield negative in-phase anomalies caused by magnetic permeability.  When magnetite is widely distributed throughout a survey area, the in-phase EM channels may continuously rise and fall, reflecting variations in the magnetite percentage, flying height, and overburden thickness.  This can lead to difficulties in recognizing deeply buried bedrock conductors, particularly if conductive overburden also exists.  However, the response of broadly distributed magnetite generally vanishes on the in-phase difference channel DIFI.  This feature can be a significant aid in the recognition of conductors that occur in rocks containing accessory magnetite.

## EM Magnetite Mapping

The information content of HEM data consists of a combination of conductive eddy current responses and magnetic permeability responses.  The secondary field resulting from conductive eddy current flow is frequency-dependent and consists of both in-phase and quadrature components, which are positive in sign.  On the other hand, the secondary field resulting from magnetic permeability is independent of frequency and consists of only an in-phase component that is negative in sign.  When magnetic permeability manifests itself by decreasing the measured amount of positive in-phase, its presence may be difficult to recognize.  However, when it manifests itself by yielding a negative in-phase anomaly (e.g., in the absence of eddy current flow), its presence is assured.  In this latter case, the negative component can be used to estimate the percent magnetite content.

A magnetite mapping technique, based on the low frequency coplanar data, can be complementary to magnetometer mapping in certain cases.  Compared to magnetometry, it is far less sensitive but is more able to resolve closely spaced magnetite zones, as well as providing an estimate of the amount of magnetite in the rock.  The method is sensitive to 1/4% magnetite by weight when the EM sensor is at a height of 30 m above a magnetitic half-space. It can individually resolve steep dipping narrow magnetite-rich bands which are separated by 60 m.  Unlike magnetometry, the EM magnetite method is unaffected by remanent magnetism or magnetic latitude.

The EM magnetite mapping technique provides estimates of magnetite content which are usually correct within a factor of 2 when the magnetite is fairly uniformly distributed.  EM

magnetite maps can be generated when magnetic permeability is evident as negative in-phase responses on the data profiles.

Like magnetometry, the EM magnetite method maps only bedrock features, provided that the overburden is characterized by a general lack of magnetite. This contrasts with resistivity mapping which portrays the combined effect of bedrock and overburden.

## The Susceptibility Effect

When the host rock is conductive, the positive conductivity response will usually dominate the secondary field, and the susceptibility effect[7] will appear as a reduction in the in-phase, rather than as a negative value. The in-phase response will be lower than would be predicted by a model using zero susceptibility. At higher frequencies the in-phase conductivity response also gets larger, so a negative magnetite effect observed on the low frequency might not be observable on the higher frequencies, over the same body. The susceptibility effect is most obvious over discrete magnetite-rich zones, but also occurs over uniform geology such as a homogeneous half-space.

High magnetic susceptibility will affect the calculated apparent resistivity, if only conductivity is considered. Standard apparent resistivity algorithms use a homogeneous half-space model, with zero susceptibility. For these algorithms, the reduced in-phase response will, in most cases, make the apparent resistivity higher than it should be. It is important to note that there is nothing wrong with the data, nor is there anything wrong with the processing algorithms. The apparent difference results from the fact that the simple geological model used in processing does not match the complex geology.

## Measuring and Correcting the Magnetite Effect

Theoretically, it is possible to calculate (forward model) the combined effect of electrical conductivity and magnetic susceptibility on an EM response in all environments. The difficulty lies, however, in separating out the susceptibility effect from other geological effects when deriving resistivity and susceptibility from EM data.

Over a homogeneous half-space, there is a precise relationship between in-phase, quadrature, and altitude. These are often resolved as phase angle, amplitude, and altitude. Within a reasonable range, any two of these three parameters can be used to calculate the half space resistivity. If the rock has a positive magnetic susceptibility, the in-phase component will be reduced and this departure can be recognized by comparison to the other parameters.

---

[7] Magnetic susceptibility and permeability are two measures of the same physical property. Permeability is generally given as relative permeability, $\mu_r$, which is the permeability of the substance divided by the permeability of free space ($4\pi \times 10^{-7}$). Magnetic susceptibility $k$ is related to permeability by $k=\mu^r-1$. Susceptibility is a unitless measurement, and is usually reported in units of $10^{-6}$. The typical range of susceptibilities is –1 for quartz, 130 for pyrite, and up to $5 \times 10^5$ for magnetite, in $10^{-6}$ units (Telford et al, 1986).

The algorithm used to calculate apparent susceptibility and apparent resistivity from HEM data, uses a homogeneous half-space geological model.  Non half-space geology, such as horizontal layers or dipping sources, can also distort the perfect half-space relationship of the three data parameters.  While it may be possible to use more complex models to calculate both rock parameters, this procedure becomes very complex and time-consuming.  For basic HEM data processing, it is most practical to stick to the simplest geological model.

Magnetite reversals (reversed in-phase anomalies) have been used for many years to calculate an "FeO" or magnetite response from HEM data (Fraser, 1981).  However, this technique could only be applied to data where the in-phase was observed to be negative, which happens when susceptibility is high and conductivity is low.

## Applying Susceptibility Corrections

Resistivity calculations done with susceptibility correction may change the apparent resistivity.  High-susceptibility conductors, that were previously masked by the susceptibility effect in standard resistivity algorithms, may become evident.  In this case the susceptibility corrected apparent resistivity is a better measure of the actual resistivity of the earth.  However, other geological variations, such as a deep resistive layer, can also reduce the in-phase by the same amount.  In this case, susceptibility correction would not be the best method.  Different geological models can apply in different areas of the same data set.  The effects of susceptibility, and other effects that can create a similar response, must be considered when selecting the resistivity algorithm.

## Susceptibility from EM vs Magnetic Field Data

The response of the EM system to magnetite may not match that from a magnetometer survey.  First, HEM-derived susceptibility is a rock property measurement, like resistivity.  Magnetic data show the total magnetic field, a measure of the potential field, not the rock property.  Secondly, the shape of an anomaly depends on the shape and direction of the source magnetic field.  The electromagnetic field of HEM is much different in shape from the earth's magnetic field.  Total field magnetic anomalies are different at different magnetic latitudes; HEM susceptibility anomalies have the same shape regardless of their location on the earth.

In far northern latitudes, where the magnetic field is nearly vertical, the total magnetic field measurement over a thin vertical dike is very similar in shape to the anomaly from the HEM-derived susceptibility (a sharp peak over the body).  The same vertical dike at the magnetic equator would yield a negative magnetic anomaly, but the HEM susceptibility anomaly would show a positive susceptibility peak.

## Effects of Permeability and Dielectric Permittivity

Resistivity algorithms that assume free-space magnetic permeability and dielectric permittivity, do not yield reliable values in highly magnetic or highly resistive areas. Both magnetic polarization and displacement currents cause a decrease in the in-phase component, often resulting in negative values that yield erroneously high apparent resistivities. The effects of magnetite occur at all frequencies, but are most evident at the lowest frequency. Conversely, the negative effects of dielectric permittivity are most evident at the higher frequencies, in resistive areas.

The table below shows the effects of varying permittivity over a resistive (10,000 ohm-m) half space, at frequencies of 56,000 Hz (DIGHEM$^V$) and 102,000 Hz (RESOLVE).

### Apparent Resistivity Calculations
### Effects of Permittivity on In-phase/Quadrature/Resistivity

| Freq (Hz) | Coil | Sep (m) | Thres (ppm) | Alt (m) | In Phase | Quad Phase | App Res | App Depth (m) | Permittivity |
|---|---|---|---|---|---|---|---|---|---|
| 56,000 | CP | 6.3 | 0.1 | 30 | 7.3 | 35.3 | 10118 | -1.0 | 1 Air |
| 56,000 | CP | 6.3 | 0.1 | 30 | 3.6 | 36.6 | 19838 | -13.2 | 5 Quartz |
| 56,000 | CP | 6.3 | 0.1 | 30 | -1.1 | 38.3 | 81832 | -25.7 | 10 Epidote |
| 56,000 | CP | 6.3 | 0.1 | 30 | -10.4 | 42.3 | 76620 | -25.8 | 20 Granite |
| 56,000 | CP | 6.3 | 0.1 | 30 | -19.7 | 46.9 | 71550 | -26.0 | 30 Diabase |
| 56,000 | CP | 6.3 | 0.1 | 30 | -28.7 | 52.0 | 66787 | -26.1 | 40 Gabbro |
| 102,000 | CP | 7.86 | 0.1 | 30 | 32.5 | 117.2 | 9409 | -0.3 | 1 Air |
| 102,000 | CP | 7.86 | 0.1 | 30 | 11.7 | 127.2 | 25956 | -16.8 | 5 Quartz |
| 102,000 | CP | 7.86 | 0.1 | 30 | -14.0 | 141.6 | 97064 | -26.5 | 10 Epidote |
| 102,000 | CP | 7.86 | 0.1 | 30 | -62.9 | 176.0 | 83995 | -26.8 | 20 Granite |
| 102,000 | CP | 7.86 | 0.1 | 30 | -107.5 | 215.8 | 73320 | -27.0 | 30 Diabase |
| 102,000 | CP | 7.86 | 0.1 | 30 | -147.1 | 259.2 | 64875 | -27.2 | 40 Gabbro |

Methods have been developed (Huang and Fraser, 2000, 2001) to correct apparent resistivities for the effects of permittivity and permeability. The corrected resistivities yield more credible values than if the effects of permittivity and permeability are disregarded.

## Recognition of Culture

Cultural responses include all EM anomalies caused by man-made metallic objects. Such anomalies may be caused by inductive coupling or current gathering. The concern of the interpreter is to recognize when an EM response is due to culture. Points of consideration used by the interpreter, when coaxial and coplanar coil-pairs are operated at a common frequency, are as follows:

1.   Channels CXPL and CPPL monitor 60 Hz radiation.  An anomaly on these channels shows that the conductor is radiating power.  Such an indication is normally a guarantee that the conductor is cultural.  However, care must be taken to ensure that the conductor is not a geologic body that strikes across a power line, carrying leakage currents.

2.   A flight that crosses a "line" (e.g., fence, telephone line, etc.) yields a centre-peaked coaxial anomaly and an m-shaped coplanar anomaly.[8]  When the flight crosses the cultural line at a high angle of intersection, the amplitude ratio of coaxial/coplanar response is 2. Such an EM anomaly can only be caused by a line. The geologic body that yields anomalies most closely resembling a line is the vertically dipping thin dike.  Such a body, however, yields an amplitude ratio of 1 rather than 2. Consequently, an m-shaped coplanar anomaly with a CXI/CPI amplitude ratio of 2 is virtually a guarantee that the source is a cultural line.

3.   A flight that crosses a sphere or horizontal disk yields centre-peaked coaxial and coplanar anomalies with a CXI/CPI amplitude ratio (i.e., coaxial/coplanar) of 1/8.  In the absence of geologic bodies of this geometry, the most likely conductor is a metal roof or small fenced yard.[9]  Anomalies of this type are virtually certain to be cultural if they occur in an area of culture.

4.   A flight that crosses a horizontal rectangular body or wide ribbon yields an m-shaped coaxial anomaly and a centre-peaked coplanar anomaly.  In the absence of geologic bodies of this geometry, the most likely conductor is a large fenced area.[5]  Anomalies of this type are virtually certain to be cultural if they occur in an area of culture.

5.   EM anomalies that coincide with culture, as seen on the camera film or video display, are usually caused by culture.  However, care is taken with such coincidences because a geologic conductor could occur beneath a fence, for example.  In this example, the fence would be expected to yield an m-shaped coplanar anomaly as in case #2 above.  If, instead, a centre-peaked coplanar anomaly occurred, there would be concern that a thick geologic conductor coincided with the cultural line.

6.   The above description of anomaly shapes is valid when the culture is not conductively coupled to the environment.  In this case, the anomalies arise from inductive coupling to the EM transmitter.  However, when the environment is quite conductive (e.g., less than 100 ohm-m at 900 Hz), the cultural conductor may be conductively coupled to the environment.  In this latter case, the anomaly shapes tend to be governed by current gathering.  Current gathering can completely distort

---

[8]   See Figure C-1 presented earlier.

[9]   It is a characteristic of EM that geometrically similar anomalies are obtained from: (1) a planar conductor, and (2) a wire which forms a loop having dimensions identical to the perimeter of the equivalent planar conductor.

the anomaly shapes, thereby complicating the identification of cultural anomalies. In such circumstances, the interpreter can only rely on the radiation channels and on the camera film or video records.

# Magnetic Responses

The measured total magnetic field provides information on the magnetic properties of the earth materials in the survey area. The information can be used to locate magnetic bodies of direct interest for exploration, and for structural and lithological mapping.

The total magnetic field response reflects the abundance of magnetic material in the source. Magnetite is the most common magnetic mineral. Other minerals such as ilmenite, pyrrhotite, franklinite, chromite, hematite, arsenopyrite, limonite and pyrite are also magnetic, but to a lesser extent than magnetite on average.

In some geological environments, an EM anomaly with magnetic correlation has a greater likelihood of being produced by sulphides than one which is non-magnetic. However, sulphide ore bodies may be non-magnetic (e.g., the Kidd Creek deposit near Timmins, Canada) as well as magnetic (e.g., the Mattabi deposit near Sturgeon Lake, Canada).

Iron ore deposits will be anomalously magnetic in comparison to surrounding rock due to the concentration of iron minerals such as magnetite, ilmenite and hematite.

Changes in magnetic susceptibility often allow rock units to be differentiated based on the total field magnetic response. Geophysical classifications may differ from geological classifications if various magnetite levels exist within one general geological classification. Geometric considerations of the source such as shape, dip and depth, inclination of the earth's field and remanent magnetization will complicate such an analysis.

In general, mafic lithologies contain more magnetite and are therefore more magnetic than many sediments which tend to be weakly magnetic. Metamorphism and alteration can also increase or decrease the magnetization of a rock unit.

Textural differences on a total field magnetic contour, colour or shadow map due to the frequency of activity of the magnetic parameter resulting from inhomogeneities in the distribution of magnetite within the rock, may define certain lithologies. For example, near surface volcanics may display highly complex contour patterns with little line-to-line correlation.

Rock units may be differentiated based on the plan shapes of their total field magnetic responses. Mafic intrusive plugs can appear as isolated "bulls-eye" anomalies. Granitic intrusives appear as sub-circular zones, and may have contrasting rings due to contact metamorphism. Generally, granitic terrain will lack a pronounced strike direction, although granite gneiss may display strike.

Linear north-south units are theoretically not well-defined on total field magnetic maps in equatorial regions due to the low inclination of the earth's magnetic field. However, most stratigraphic units will have variations in composition along strike that will cause the units to appear as a series of alternating magnetic highs and lows.

Faults and shear zones may be characterized by alteration that causes destruction of magnetite (e.g., weathering) that produces a contrast with surrounding rock. Structural breaks may be filled by magnetite-rich, fracture filling material as is the case with diabase dikes, or by non-magnetic felsic material.

Faulting can also be identified by patterns in the magnetic total field contours or colours. Faults and dikes tend to appear as lineaments and often have strike lengths of several kilometres. Offsets in narrow, magnetic, stratigraphic trends also delineate structure. Sharp contrasts in magnetic lithologies may arise due to large displacements along strike-slip or dip-slip faults.

_____


**APPENDIX D**


**DATA ARCHIVE DESCRIPTION**


_____

```
                   Geosoft XYZ ARCHIVE SUMMARY
                   ---------------------------


  JOB #             :03091
  TYPE OF SURVEY    :EM, MAGNETICS, RESISTIVITY
  AREA              :Kotcho Area, BC
  CLIENT            :British Columbia Geological Survey


  **************************************************************************

  SURVEY DATA FORMAT:
  -------------------

  NUMBER OF DATA FIELDS :   49

   # CHANNAME         TIME  UNITS  DESCRIPTION
   1 X                0.10  m      UTME-NAD83
   2 Y                0.10  m      UTMN-NAD83
   3 Z                0.10  m      Height above sea level
   4 FID              1.00  n/a    Synchronization Counter
   5 LINE             0.10  n/a    Line number
   6 FLIGHT           0.10  n/a    Flight Number
   7 ALTBIRDM         0.10  m      Radar Altimeter EM Bird to Earth-Surface
   8 LASER            0.10  m      Laser Altimeter EM Bird to Earth-Surface
   9 L100I            0.10  ppm    coplanar inphase 114940 kHz RAW
  10 L1K5I            0.10  ppm    coplanar inphase 1574 Hz RAW
  11 L25KI            0.10  ppm    coplanar inphase 25300 Hz RAW
  12 L400I            0.10  ppm    coplanar inphase 389 Hz RAW
  13 L6K2I            0.10  ppm    coplanar inphase 6075 Hz RAW
  14 L1K7I            0.10  ppm    coaxial inphase 3245 Hz RAW
  15 L100Q            0.10  ppm    coplanar quadrature 114940 kHz RAW
  16 L1K5Q            0.10  ppm    coplanar quadrature 1574 Hz RAW
  17 L25KQ            0.10  ppm    coplanar quadrature 25300 Hz RAW
  18 L400Q            0.10  ppm    coplanar quadrature 389 Hz RAW
  19 L6K2Q            0.10  ppm    coplanar quadrature 6075 Hz RAW
  20 L1K7Q            0.10  ppm    coaxial quadrature 3245 Hz RAW
  21 CPI400           0.10  ppm    coplanar inphase 389 Hz
  22 CPQ400           0.10  ppm    coplanar quadrature 389 Hz
  23 CXI3300          0.10  ppm    coaxial inphase 3245 Hz
  24 CXQ3300          0.10  ppm    coaxial quadrature 3245 Hz
  25 CPI1500          0.10  ppm    coplanar inphase 1574 Hz
  26 CPQ1500          0.10  ppm    coplanar quadrature 1574 Hz
  27 CPI6200          0.10  ppm    coplanar inphase 6075 Hz
  28 CPQ6200          0.10  ppm    coplanar quadrature 6075 Hz
  29 CPI25K           0.10  ppm    coplanar inphase 25300 Hz
  30 CPQ25K           0.10  ppm    coplanar quadrature 25300 Hz
  31 CPI115K          0.10  ppm    coplanar inphase 114940 Hz
  32 CPQ115K          0.10  ppm    coplanar quadrature 114940 Hz
  33 RES400           0.10  ohm·m  Apparent Resistivity 389 Hz
  34 RES3300          0.10  ohm·m  Apparent Resistivity 3245 Hz
  35 RES1500          0.10  ohm·m  Apparent Resistivity 1574 Hz
  36 RES6200          0.10  ohm·m  Apparent Resistivity 6075 Hz
  37 RES25K           0.10  ohm·m  Apparent Resistivity 25300 Hz
  38 RES115K          0.10  ohm·m  Apparent Resistivity 114940 Hz
  39 DEP400           0.10  m      Apparent Depth 389 Hz
  40 DEP3300          0.10  m      Apparent Depth 3245 Hz
  41 DEP1500          0.10  m      Apparent Depth 1574 Hz
  42 DEP6200          0.10  m      Apparent Depth 6075 Hz
  43 DEP25K           0.10  m      Apparent Depth 25300 Hz
  44 DEP115K          0.10  m      Apparent Depth 114940 Hz
  45 MAGRD            0.10  nT     Uncorrected Total Magnetic, right sensor
  46 MAGLD            0.10  nT     Uncorrected Total Magnetic, left sensor
  47 DIURNAL          0.10  nT     Daily Variations of Magnetic Field
  48 TMI              0.10  nT     Total Magnetic Intensity from right sensor
  49 TOPO             0.10  m      Digital Terrain Model
  **************************************************************************
```

```
ISSUE DATE        :January 6, 2003
FOR WHOM          :British Columbia Geological Survey

BY  WHOM          :FUGRO AIRBORNE SURVEYS CORP.
                   2270 ARGENTIA ROAD
                   MISSISSAUGA, ONTARIO,
                   CANADA  L5N 6A6
                   TEL. (905) 812-0212
                   FAX  (905) 812-1504
```